Article

Cell Reports

The Host Protein Reticulon 3.1A Is Utilized by Flaviviruses to Facilitate Membrane Remodelling

Graphical Abstract

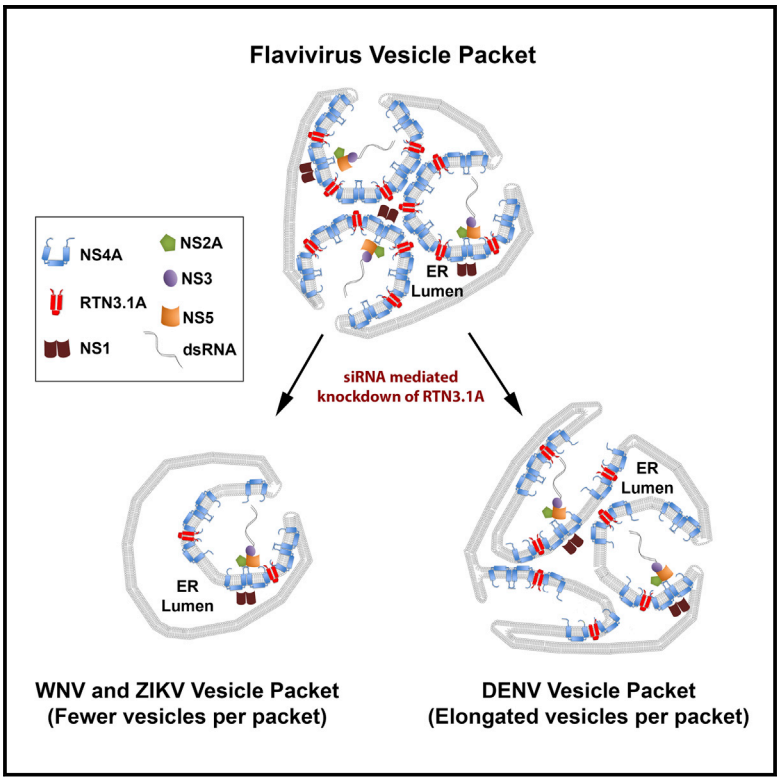

Highlights

- Flavivirus sites of replication accumulate the host remodelling protein RTN3.1A
- siRNA silencing of RTN3.1A impairs virus replication and membrane morphogenesis
- RTN3.1A interacts with the WNV_{KUN} NS4A protein to promote membrane remodelling
- Flaviviruses utilize RTN3.1A differently during their replication cycles

Authors

Turgut E. Aktepe, Susann Liebscher, Julia E. Prier, Cameron P. Simmons, Jason M. Mackenzie

Correspondence

jason.mackenzie@unimelb.edu.au

In Brief

To study the underlying mechanism of flavivirus replication and membrane biogenesis, Aktepe et al. examine the role of the host membrane-shaping protein RTN3.1A during WNV_{KUN}, $DENV\text{-}2_{NGC}$, and $ZIKV_{AFR}$ replication. They find that RTN3.1A is required for NS4A-mediated membrane remodelling during biogenesis of the flavivirus replication complex.

Aktepe et al., 2017, Cell Reports *21*, 1639–1654
November 7, 2017
https://doi.org/10.1016/j.celrep.2017.10.055

CellPress

Cell Reports
Article

The Host Protein Reticulon 3.1A Is Utilized by Flaviviruses to Facilitate Membrane Remodelling

Turgut E. Aktepe,[1] Susann Liebscher,[1] Julia E. Prier,[1] Cameron P. Simmons,[1] and Jason M. Mackenzie[1,2,*]
[1]Department of Microbiology and Immunology, University of Melbourne at the Peter Doherty Institute for Infection and Immunity, Melbourne, VIC 3000, Australia
[2]Lead Contact
*Correspondence: jason.mackenzie@unimelb.edu.au
https://doi.org/10.1016/j.celrep.2017.10.055

SUMMARY

Flaviviruses are enveloped, positive-sensed single-stranded RNA viruses that remodel host membranes, incorporating both viral and host factors facilitating viral replication. In this study, we identified a key role for the membrane-bending host protein Reticulon 3.1 (RTN3.1A) during the replication cycle of three flaviviruses: West Nile virus (WNV), Dengue virus (DENV), and Zika virus (ZIKV). We observed that, during infection, RTN3.1A is redistributed and recruited to the viral replication complex, a recruitment facilitated via the WNV NS4A protein, however, not DENV or ZIKV NS4A. Critically, small interfering RNA (siRNA)-mediated knockdown of RTN3.1A expression attenuated WNV, DENV, and ZIKV replication and severely affected the stability and abundance of the NS4A protein, coinciding with a significant alternation and reduction of viral membrane structures in the endoplasmic reticulum. These observations identified a crucial role of RTN3.1A for the viral remodelling of host membranes during efficient flavivirus replication and the stabilization of viral proteins within the endoplasmic reticulum.

INTRODUCTION

The *Flaviviridae* family contains numerous highly pathogenic viruses, such as West Nile virus (WNV), Dengue virus (DENV), Zika virus (ZIKV), Japanese encephalitis virus (JEV), and Yellow Fever virus (YFV). To successfully replicate its small genome size (~11 kb), flaviviruses utilize both viral and host factors to aid in transcription, translation, immune evasion, and remodelling of the intracellular membranous environment (Romero-Brey and Bartenschlager, 2016). This remodelling of membranes drives the biogenesis of characteristic flavivirus-induced membrane structures that are highly curved and complex, termed vesicle packets (VPs), convoluted membrane (CM), and paracrystalline arrays (PCs) (Westaway et al., 1997; Mackenzie et al., 1996). Previous studies by multiple groups have identified that these membrane structures are derived from the endoplasmic reticulum (ER) and also contain markers of the Golgi apparatus (Welsch et al., 2009; Gillespie et al., 2010; Mackenzie et al., 1999; Miorin et al., 2013; Junjhon et al., 2014; Cortese et al., 2017). These membrane structures act as platforms for efficient viral replication by compartmentalizing and hiding viral components from innate immune detection (Hoenen et al., 2007; Overby et al., 2010; Hoenen et al., 2014); however, the exact mechanism underlying the formation of these structures is not entirely understood (Mackenzie et al., 1999; Westaway et al., 1997; Gillespie et al., 2010; Welsch et al., 2009).

Viral replication is a complex process that requires many host factors at every stage of replication, including the formation of virally induced membrane structures (Ahlquist et al., 2003; Wang and Li, 2012). It is now well established that the proliferation of intracellular membranes during WNV and DENV replication is mediated via the small hydrophobic protein NS4A, which, when individually expressed, is sufficient to proliferate membranes similar to the CM/PC observed during viral replication (Miller et al., 2007; Roosendaal et al., 2006). NS4A is a 16-kDa highly hydrophobic, ER-associated protein with three transmembrane (TM) regions, a membrane-associated region, and an N-terminal cytoplasmic region (Mackenzie et al., 1998b; Miller et al., 2007). NS4A is also predicted to form part of the replication complex (RC), determined from studies that have shown interactions with the replicative intermediates double-stranded RNA (dsRNA), NS1, NS2A, and NS5 (Mackenzie et al., 1998a) and via its interaction with the cellular scaffolding protein vimentin to aid RC formation (Teo and Chu, 2014). Additionally, mutations within the conserved amino acid and TM domains of NS4A impacted negatively on NS4A protein stability, cleavage efficiency, and oligomerization and duly on virus replication (Ambrose and Mackenzie, 2011a, 2015; Stern et al., 2013; Lee et al., 2015).

The Reticulon (RTN) protein family is a large group of membrane-associated proteins that are involved in vesicle formation and membrane morphogenesis. The RTN protein family consists of four gene products (*RTN1*, *RTN2*, *RTN3*, and *RTN4/Nogo*), and, further, depending on promoters and alternative splicing, it includes more than 300 proteins (Oertle et al., 2003; Moreira et al., 1999). A common feature of all RTN proteins is the C-terminal Reticulon Homology Domain (RHD) that consists of two hairpin TM regions separated by a hydrophilic loop. The short topology of the hairpin TM sits on the outer leaflet of the ER membrane and occupies a higher density of space, causing a positive curvature of the membrane toward the cytoplasm (Yang and Strittmatter, 2007; Zurek et al., 2011). The RTN proteins localize to regions with high membrane curvature, and they are required

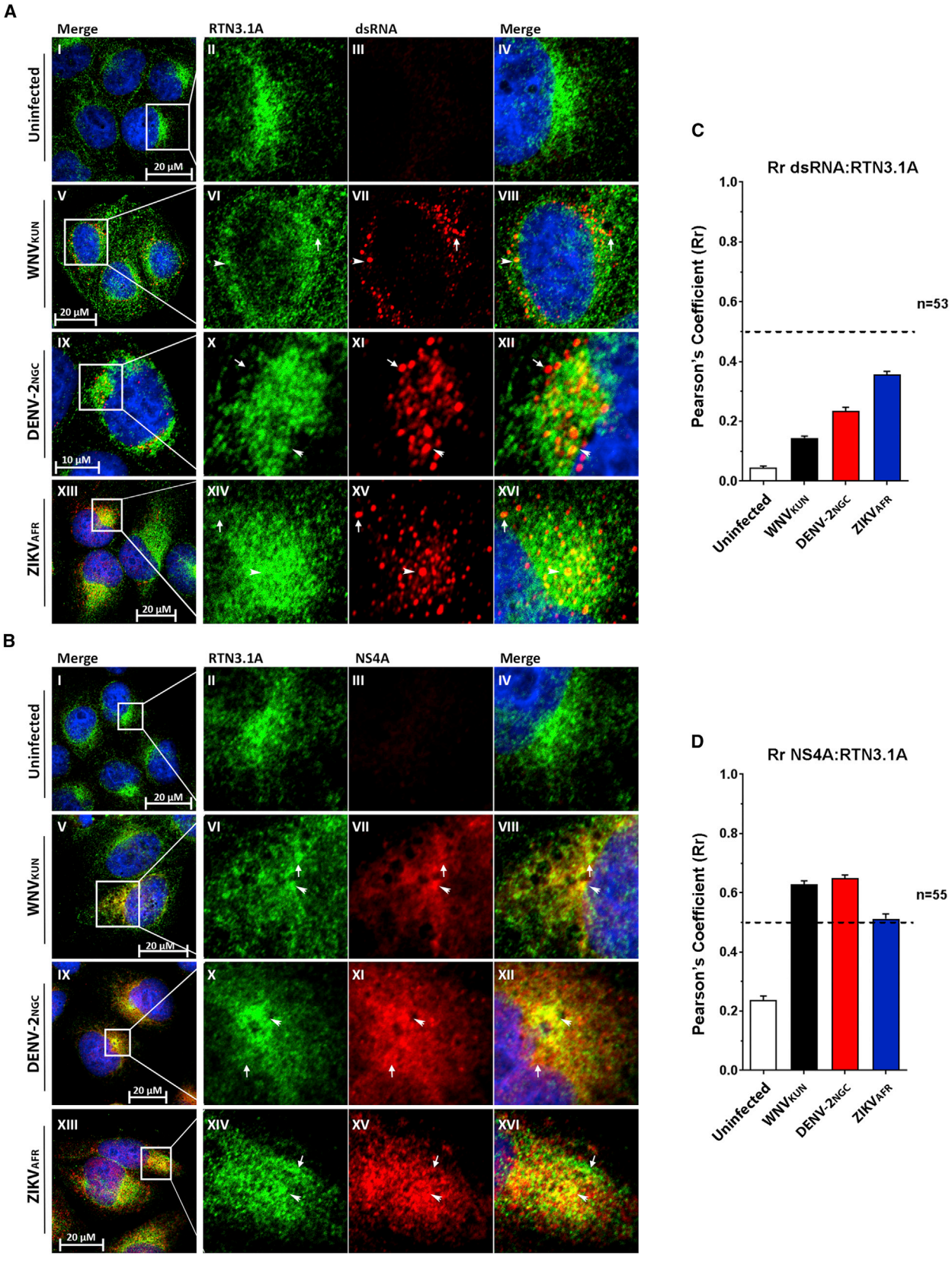

(legend on next page)

to control the formation of ER tubules and increase peripheral ER sheets (Voeltz et al., 2006; Tolley et al., 2010; Westrate et al., 2015). Previous studies have suggested a differential requirement of RTN proteins during the replication of +single-stranded RNA (ssRNA) virus replication. Enterovirus 71 (EV71) requires RTN3A for replication as knockdown of RTN3A (via RNAi) inhibited EV71 replication (Tang et al., 2007). Additionally, it was shown that the EV71 2C protein directly interacts with RTN3A to promote efficient replication (Tang et al., 2007). Similarly, the brome mosaic virus (BMV) 1a protein interacts with and incorporates RTN proteins into the virus-induced spherules (comprising the RC), and deletion of a number of RTN proteins attenuated BMV replication (Diaz et al., 2010). In contrast, RTN3A interacts with and negatively regulates Hepatitis C virus (HCV) NS4B dimerization, and silencing of RTN3A enhanced HCV replication (Barajas et al., 2014).

Based on the observations described above, we aimed to determine the role and impact of RTN3.1A on flavivirus replication, and we demonstrated that RTN3.1A is required for the efficient replication of WNV strain Kunjin (WNV_{KUN}), DENV-2 strain New Guinea-C (DENV-2_{NGC}), and ZIKV African MR766 strain ($ZIKV_{AFR}$). Ultimately, we have demonstrated that flaviviruses utilize the membrane-bending capacity of the viral NS4A protein and the host RTN3.1A protein in concert to generate the viral VP and CM/PC required for efficient viral replication. The data presented in this study provide insight into the virus-host interactions that drive flavivirus replication.

RESULTS

WNV_{KUN}, DENV-2_{NGC}, and $ZIKV_{AFR}$ Recruit RTN3.1A to the Sites of Virus Replication

RTN3.1A is a membrane-bound protein required for the bending and shaping of the ER, and it plays a critical role in the replication of many (+)RNA viruses. We sought to examine the role of RTN3.1A during flavivirus replication, as it was previously shown that enterovirus 71 and HCV utilize RTN3.1A, albeit differentially (Tang et al., 2007; Diaz et al., 2010; Barajas et al., 2014; Wu et al., 2014). In addition, it is ubiquitously expressed in different tissues, reducing the restriction of tropism and making it a potential target for flaviviruses to aid in reshaping ER membranes to house their viral replication complex. Some RTN transcripts though have tissue specificity (e.g., *RTN1* is almost exclusively expressed in neurons and neuroendocrine cells; *RTN2-C* and *RTN4-C* in skeletal muscle; and *RTN4-A* in oligodendrocytes, heart, and testis; Oertle and Schwab, 2003).

To determine the intracellular distribution of RTN3.1A during flavivirus infection, HeLa cells were infected with WNV_{KUN}, DENV-2_{NGC}, or $ZIKV_{AFR}$ and fixed for immunofluorescence (IF) analysis (Figure 1). Fixed samples were immune-labeled with antibodies to endogenous RTN3.1A and the viral markers dsRNA and the viral protein NS4A. Within uninfected cells (Figures 1A, I–IV, and 1B, I–IV), the RTN3.1A protein was observed to localize as a reticular staining pattern in the cytoplasm and also confined to the perinuclear region. This distribution is consistent with previous observations indicating that RTN3.1A resides primarily within the ER and Golgi (Kume et al., 2009). Upon infection with WNV_{KUN}, DENV-2_{NGC}, or $ZIKV_{AFR}$, dsRNA, which is a marker for viral replication complexes (Westaway et al., 1999), was observed to partially co-localize with RTN3.1A (Figures 1A, V–XVI). We observed the RTN3.1A staining as adjacent or juxtaposed to that of dsRNA (indicated by arrows), in addition to complete co-localization (indicated by arrowheads), and overall with a more pronounced association of RTN3.1A with $ZIKV_{AFR}$ dsRNA compared to DENV-2_{NGC} and WNV_{KUN} (Figure 1C).

Conversely, we observed significant co-localization between RTN3.1A and WNV_{KUN}, DENV-2_{NGC}, or $ZIKV_{AFR}$ NS4A during flavivirus replication (Figures 1B, V–XVI, and 1D). Previous studies on WNV_{KUN} and DENV-2_{NGC} have described that the NS4A protein localizes primarily to the CM/PC structures (in addition to the VP) (Mackenzie et al., 1998a; Welsch et al., 2009) and that NS4A has the intrinsic capability to remodel cytoplasmic membranes to induce CM/PC (Roosendaal et al., 2006; Miller et al., 2007). Thus, our observations here suggest that the host protein RTN3.1A is localized to modified ER membranes that comprise flavivirus replication complexes.

Silencing of RTN3.1A Expression Attenuates Flavivirus Replication and Promotes Degradation of NS4A

To determine the role of RTN3.1A during flavivirus replication, RTN3.1A expression was silenced in HEK293T cells using small interfering RNA (siRNA) targeting the *RTN3.1A* gene (Figure 2). The effects of RTN3.1A on virus replication were assessed by qRT-PCR (for genome replication), western blotting (for protein production), and plaque assay (for production of infectious virus) (Figures 2A–2C, respectively). The efficiency of RNAi-mediated silencing of RTN3.1A was assessed by western blot analysis where we observed an ~90% reduction in endogenous RTN3.1A protein levels (see Figure 2B for protein levels). Our qRT-PCR analyses of total cellular RNA revealed that depletion of RTN3.1A did not affect the production of either WNV_{KUN} (−) sense or (+) sense RNA at the transcriptional level (Figure 2A, i). However, silencing of RTN3.1A resulted in an ~1.5 $\log_{10}$ decrease in DENV-2_{NGC} (−) sense RNA and an ~0.5 $\log_{10}$ decrease in (+) sense RNA and an ~1 $\log_{10}$ decrease in $ZIKV_{AFR}$ (−) sense RNA and an ~0.5 $\log_{10}$ decrease in (+) sense RNA compared to control siRNA-treated, infected cells (Figure 2A, ii and iii, respectively).

Figure 1. Flaviviruses Recruit the Host Protein RTN3.1A to the Site of Virus Replication

(A and B) HeLa cells were mock (I–IV), WNV_{KUN} (V–VIII), DENV-2_{NGC} (IX–XII), or $ZIKV_{AFR}$ (XIII–XVI) infected; fixed at 24, 36, and 48 hr post-infection (h.p.i.), respectively; and immunolabeled with antibodies to the host protein RTN3.1A (green; II, VI, X, and XIV) or (A) the viral components dsRNA (red; III, VII, XI, and XV) or (B) NS4A protein (red; III, VII, XI, and XV). The merged images are provided in both low (I, V, IX, and XIII) and high (IV, VIII, XII, and XVI) magnification with a yellow hue and arrowheads that indicate regions of co-localization.

(C and D) Pearson's coefficient (co-localization) between (C) dsRNA and RTN3.1A and (D) NS4A and RTN3.1A is graphically depicted and was determined by the JaCOP plugin software in ImageJ on multiple images collected over replicate experiments. Error bars indicate mean *Rr* ± SEM. Images were acquired using the Zeiss LSM710 confocal microscope.

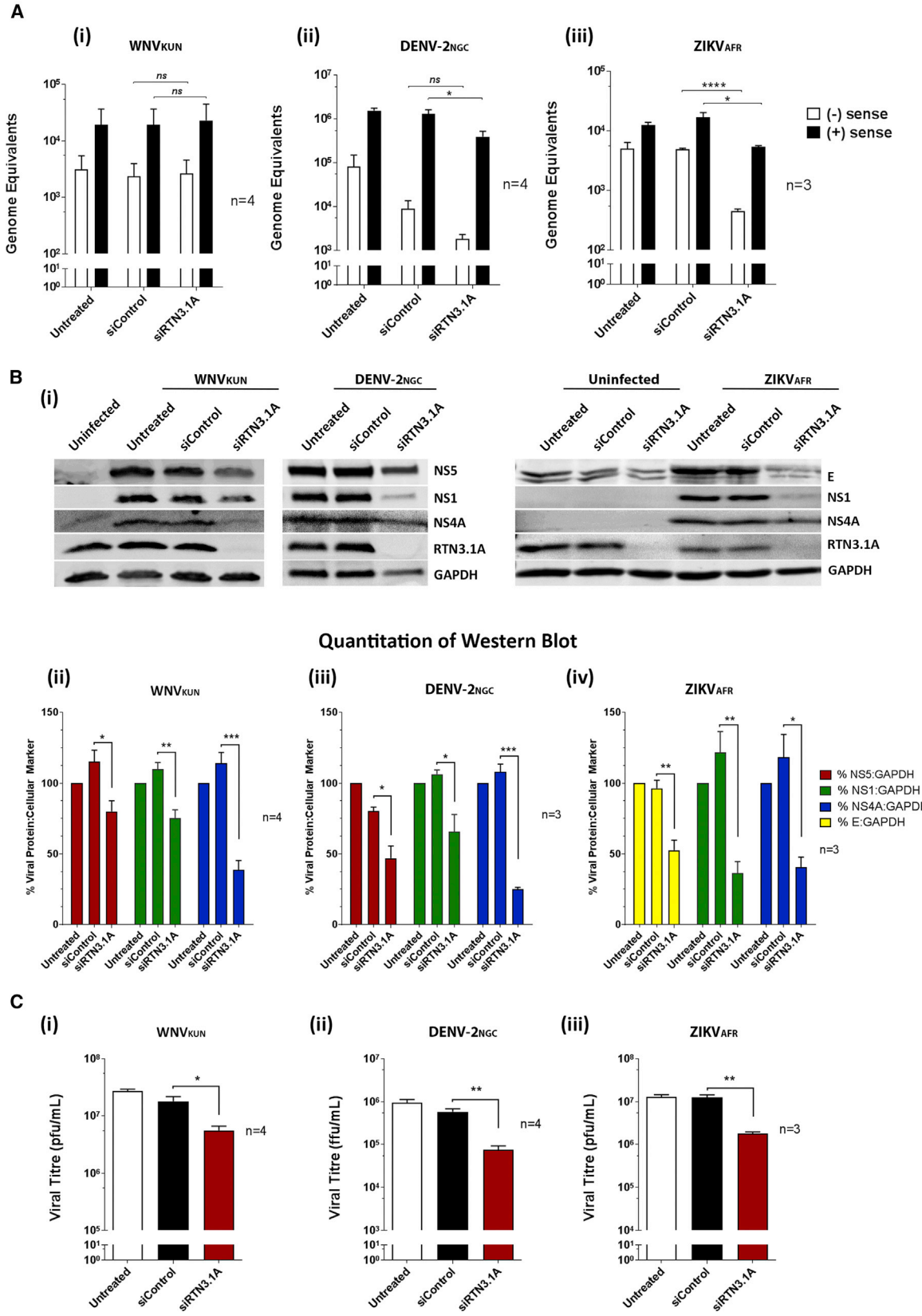

(legend on next page)

We subsequently analyzed whole-cell lysates from RTN3.1A-silenced and virus-infected cells by western blot, and we observed an ~25% reduction in both WNV_{KUN} NS1 and NS5 protein levels in the RTN3.1A knockdown cells compared to control siRNA-treated, infected cells (Figure 2B, i and ii). Surprisingly, even though the flavivirus genome is translated off a single open reading frame, we additionally observed an ~65% reduction in the amount of NS4A protein in the RTN3.1A-silenced cells compared to untreated cells (Figure 2B, i and ii). These observations were confirmed upon DENV-2_{NGC} infection of RTN3.1A-silenced cells, where again we observed ~50%, ~35%, and ~70% decreases in DENV-2_{NGC} NS5, NS1, and NS4A protein levels, respectively (Figure 2B, i and iii). Intriguingly, $ZIKV_{AFR}$ infection of the RTN3.1A-depleted cells produced an ~50% decrease in E protein and an ~60% decrease in NS1 and NS4A proteins. In contrast to WNV_{KUN} and DENV-2_{NGC}, the extent of NS4A reduction, however, was similar to the other viral proteins (Figure 2B, i and iv). In agreement with our observed reductions in flavivirus RNA and protein level upon RTN3.1A depletion, we additionally observed a corresponding ~0.5 $\log_{10}$ decrease in WNV_{KUN} and ~1.0 $\log_{10}$ reduction in DENV-2_{NGC} and $ZIKV_{AFR}$ viral titer (Figure 2C, i–iii).

Overall these results highlight the importance of the host protein RTN3.1A in the replication of flaviviruses. Furthermore, in the absence of RTN3.1A, the levels of the WNV_{KUN} and DENV-2_{NGC} NS4A protein was greatly decreased, with respect to the other viral proteins. Thus, it is apparent that WNV_{KUN}, DENV-2_{NGC}, and $ZIKV_{AFR}$ all utilize RTN3.1A but with subtle differences during their replication cycles.

RNAi-Mediated Silencing of RTN3.1A Expression Reduces Flavivirus-Induced Membrane Remodelling

Previous studies have revealed that the flavivirus NS4A protein plays a significant role in the observed remodelling of cytoplasmic membranes and that specific mutations within NS4A increase protein degradation, thus duly affecting membrane remodelling (Roosendaal et al., 2006; Miller et al., 2007; Ambrose and Mackenzie, 2015). As we had observed that RNAi-mediated silencing of RTN3.1A expression also resulted in reduced NS4A, we sought to determine if this also affected the ability of each of the flaviviruses to remodel intracellular membranes (Figures 3, 4, and 5).

Initially, we evaluated the effect of RTN3.1A silencing on the ER membrane ultrastructure in HEK293T cells via transmission electron microscopy, and we observed minimal effect on cell viability and on the curvature of ER membranes in RTN3.1A-silenced and control siRNA-treated cells (Figure S1). In subsequent experiments, HEK293T cells were treated with RNAi targeting the *RTN3.1A* gene and infected with WNV_{KUN}, DENV-2_{NGC}, or $ZIKV_{AFR}$. In cells that were untreated but infected, we observed membrane alterations characteristic of WNV_{KUN}, DENV-2_{NGC}, and $ZIKV_{AFR}$ infection (Figures 3, 4, and 5). For WNV_{KUN}, these included clustered replication vesicles (VPs), CM/PC structures, and the presence of virus particles (Figures 3A and 3B). For DENV-2_{NGC} and $ZIKV_{AFR}$, these were identified as the formation of single as well as clustered replication vesicles (Figures 4A–4C and 5A–5C, respectively). CMs could also be observed in DENV-2_{NGC}- and $ZIKV_{AFR}$-infected cells; however, these were less frequently observed than during WNV_{KUN} infection. All three viruses induced an expansion of the ER lumen, especially $ZIKV_{AFR}$ that produced greatly enlarged ER and large vacuoles within the cytoplasm (Figure 5). Virus particles were observed within the ER lumen and throughout the trans-Golgi network as single particles or as virus stacks for all three flaviviruses (Figures 3, 4, and 5).

Analogous morphology and virus particles were also observed within cells treated with the control RNAi and infected with the different flaviviruses (Figures 3C, 3D, 4D–4F, and 5D–5F). In contrast, we detected a drastic effect on virus-induced membrane structures in the RTN3.1A-depleted cells, which differed among the three flaviviruses. In RTN3.1A-silenced and WNV_{KUN}-infected cells, we observed a significant reduction in membrane alterations, solely small or no CM/PCs, and infrequent single replication vesicles (Figures 3E and 3F). Our quantitative analyses revealed that, upon RTN3.1A silencing, the area of the WNV_{KUN}-induced CM/PC membrane structures (Figure 3G) alongside the number of virus-induced vesicles per infected cell (Figure 3H) was significantly reduced, indicating a decreased viral replication fitness for WNV_{KUN} in RTN3.1-depleted cells.

Interestingly, during DENV-2_{NGC} infection (Figure 4), we observed a different effect of RTN3.1A silencing on virus-induced membrane structures than in WNV_{KUN}-infected cells. In RTN3.1A-silenced DENV-2_{NGC}-infected cells, we observed that the replication vesicles within the VP were more elongated (Figures 4G–4I, arrows) in comparison to untreated and siRNA-control-treated cells (Figures 4A–4F); however, the quantity of vesicles did not appear to be altered. We evaluated the vesicle diameters, and we observed that untreated and control siRNA-treated vesicles were of similar size, ranging from 93.6 ± 12.5 nm (minimum 64.1 nm/maximum 128.0 nm) and 93.4 ± 16.0 nm (minimum 63.1 nm/maximum 140.9 nm), respectively. In contrast, the average vesicle length in DENV-2_{NGC}-infected RTN3.1A-silenced cells was 106.4 ± 26.8 nm, with a significantly

Figure 2. siRNA-Mediated Reduction in RTN3.1A Expression Attenuates Flavivirus Protein and Virus Production

HeLa cells were untreated or treated with control siRNA or siRNA specific for the host *RTN3.1A* gene; infected with WNV_{KUN}, DENV-2_{NGC}, and $ZIKV_{AFR}$; and viral RNA, whole-cell lysates, and extracellular virus were collected.

(A) RNA samples were analyzed for WNV_{KUN} (i), DENV-2_{NGC} (ii), and $ZIKV_{AFR}$ (iii) genome levels using qPCR (WNV_{KUN} and DENV-2_{NGC} n = 4 and $ZIKV_{AFR}$ n = 3).

(B) Protein lysates were analyzed by western blot (i) using antibodies raised against WNV_{KUN} and DENV-2_{NGC} NS5, NS1, and NS4A protein; $ZIKV_{AFR}$ E, NS1, and NS4A proteins; the host proteins RTN3.1A; and GAPDH (ii–iv). Quantitations over replicate experiments are provided (WNV_{KUN} n = 4, DENV-2_{NGC}, and $ZIKV_{AFR}$ n = 3).

(C) Cell culture supernatants were analyzed for infectious virus production during siRNA-mediated silencing by plaque assay (WNV_{KUN} [i] and DENV-2_{NGC} [ii] n = 4 and $ZIKV_{AFR}$ [iii] n = 3). In all cases, error bars indicate mean ± SEM of replicate analysis of replicate experiments. Significant changes are indicated and were determined by Student's t test (GraphPad Prism 6).

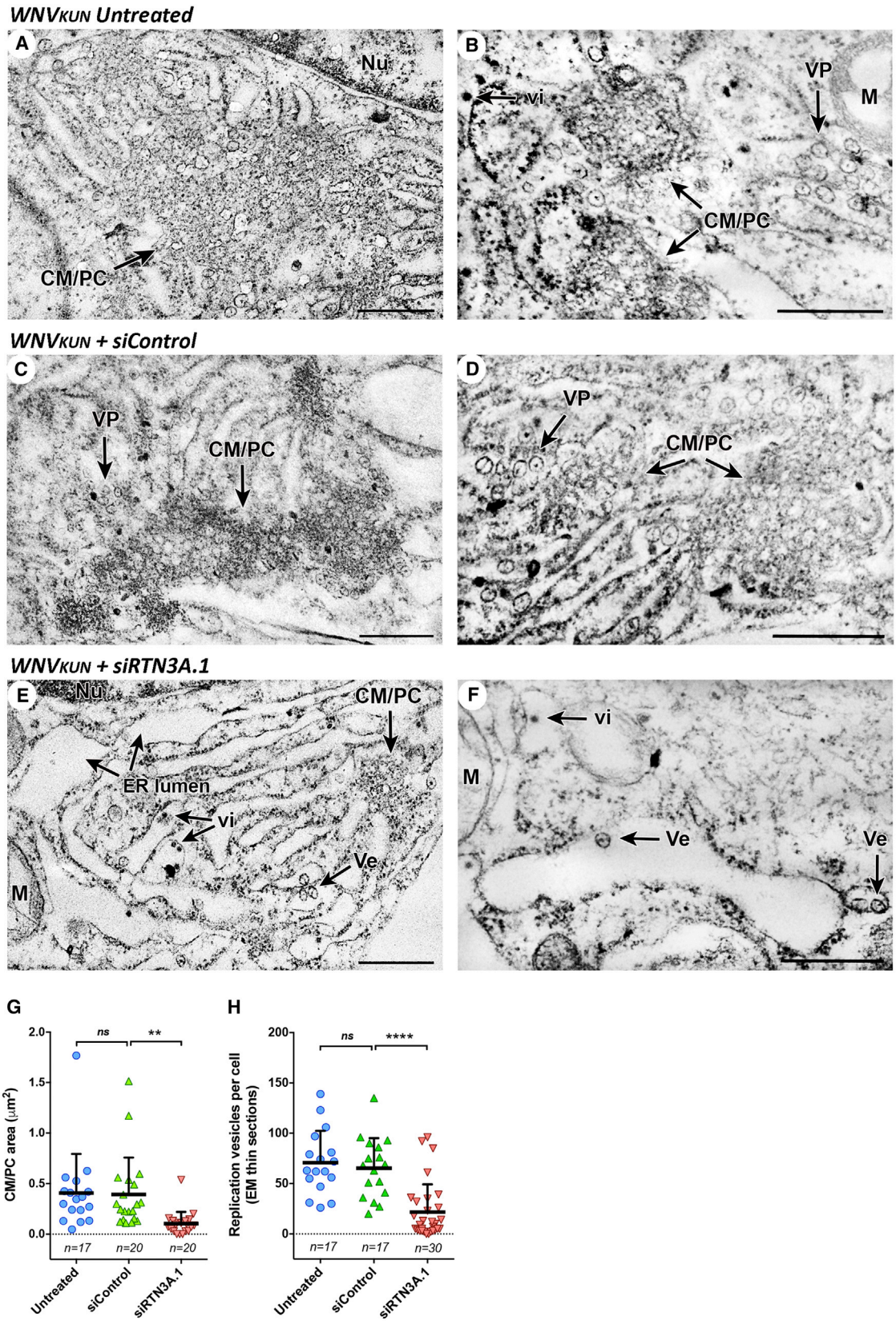

(legend on next page)

larger range from a minimum vesicle length of 58.0 nm up to a maximum vesicle length of 220.1 nm (Figure 4J). Additionally, we observed a significantly highly proportion of fuzzy-coated DENV-2_{NGC} particles in the RTN3.1A-depleted cells (Figure 4M) compared to the smooth appearance of these particles in untreated (Figure 4K) and control siRNA-treated and DENV-2_{NGC}-infected cells (Figure 4L). These observations indicate that RTN3.1A depletion increased the number of immature virus particles.

Furthermore, in RTN3.1A-silenced $ZIKV_{AFR}$-infected cells, we detected a low number of replication vesicles and a proliferated ER that displayed less membrane curvature (Figures 5G and 5H) than in natural $ZIKV_{AFR}$ infections (compare to Figures 5A–5C). Most commonly, we only observed single virus particles within the expanded ER (vacuoles) without detectable replication complexes (Figures 5I and 5J). Quantitative analysis indicated a significant decrease in the number of replication vesicles per electron microscopy (EM) thin section per infected cell (Figure 5K), suggesting that RTN3.1A silencing dramatically reduced the capacity of $ZIKV_{AFR}$ to remodel ER membranes.

Overall, these ultrastructural observations indicate that RTN3.1A contributes to the formation of flavivirus-typical ER membranes to promote efficient virus replication, potentially in concert with the membrane-remodelling capability of NS4A. However, the utilization of the RTN3.1A protein appears to differ among the three flaviviruses.

Silencing of RTN3.1A Promotes the Degradation of Viral Proteins

Previously we had observed that silencing of RTN3.1A resulted in a significant decrease in viral protein abundance, particularly the NS4A protein. To assess this further, flow cytometry analysis was performed in HEK293T cells that were untransfected or transfected with siRNA-control or siRNA-RTN3.1A, followed by transfection of recombinant plasmids expressing GFP, NS4B-GFP, WNV_{KUN}, DENV-2_{NGC}, and $ZIKV_{AFR}$ GFP-NS4A(−2K) proteins (Figure 6). Analysis of the GFP mean fluorescence intensity (MFI) revealed that siRNA-mediated silencing of RTN3.1A did not significantly reduce GFP alone, although the expression was reduced to some extent (Figure 6A). However, upon RTN3.1A silencing, we observed a significant reduction in NS4B-GFP MFI levels (Figure 6A), with a greater reduction in WNV_{KUN}, DENV-2_{NGC}, and $ZIKV_{AFR}$ GFP-NS4A(−2K) MFI levels (Figure 6A).

The cellular proteasome is responsible for the degradation of intracellular proteins (Tanaka, 2009). To disentangle the role of the proteasome in viral protein degradation, we utilized four proteasome inhibitors (carfilzomib [0.5 μM], MG-132 [0.5 μM], eeyarestatin I [10 μM], and bortezomib [10 nM]) and DMSO as a solvent control (0.1% DMSO) to determine if viral protein levels could be restored upon proteasome inhibition (Figures 6B–6F). Intriguingly, we observed that proteasome inhibition with carfilzomib and MG-132 partially restored WNV_{KUN} NS4B-GFP and WNV_{KUN}, DENV-2_{NGC}, and $ZIKV_{AFR}$ GFP-NS4A(−2K) levels in comparison to siRNA-control (Figures 6C and 6D). However, treatment with eeyarestatin I or bortezomib did not restore viral protein levels to siRNA-control (Figures 6C and 6D).

These observations suggest that the suppression of RTN3.1A impacts on the degradation of viral proteins, and we have demonstrated that this reduction may be due to the proteolytic activity of the 20S subunit of the host proteasome. However, we could not restore the expression levels to 100%, indicating that the proteasome cannot be the only contributing factor. Our results would intimate that an additional role for RTN3.1A is to ensure the stability of viral proteins within the ER.

RTN3.1A Specifically Co-localizes and Interacts with WNV_{KUN} NS4A

Our previous observations indicated that RTN3.1A co-localized with flavivirus NS4A protein and that depletion of RTN3.1A resulted in a major reduction of WNV_{KUN} and DENV-2_{NGC} NS4A compared to other viral proteins. Thus, we aimed to determine if RTN3.1A specifically interacted with the flavivirus protein NS4A by IF analysis. To investigate this, we initially screened the distribution and co-localization of endogenous RTN3.1A with transiently expressed recombinant WNV_{KUN}, DENV-2_{NGC}, and $ZIKV_{AFR}$ GFP-NS4A(−2K) and the WNV_{KUN} NS4B-GFP constructs.(Figure 7A). We observed that, as previously, the distribution of RTN3.1A was diffuse within the cytoplasm but did appear to accumulate in the perinuclear region in mock-transfected cells (Figure 7A, I–IV). Further, we observed that transfection of all recombinant flavivirus proteins did induce changes in RTN3.1A distribution to a more discrete punctate-like pattern (Figure 7A, III compared to VII, XI, XV, and XIX); however, co-localization was only observed with the WNV_{KUN} GFP-NS4A(−2K) proteins (Figure 7A, IX–XII, arrowheads; $Rr = 0.72 \pm 0.02$). Although DENV-2_{NGC} and $ZIKV_{AFR}$ GFP-NS4A(−2K) appeared to co-localize with RTN3.1A (Figure 7A, XVI and XX, arrowheads; $Rr = 0.42 \pm 0.02$ and $Rr = 0.40 \pm 0.01$, respectively), most of the RTN3.1A localization appeared to be adjacent or juxtaposed to GFP (Figure 7A, XVI and XX, arrows).

Figure 3. siRNA-Mediated Transient Silencing of RTN3.1A Expression Attenuates the Capacity of WNV_{KUN} to Remodel Cytoplasmic Membranes

(A–F) HEK293T cells were untreated (A and B) or treated with control siRNA (C and D) or siRNA specific for the host *RTN3.1A* gene (E and F) prior to WNV_{KUN} infection. At 24 h.p.i. the cells were harvested and processed for EM analysis. (A and B) Untreated WNV_{KUN}-infected cells are shown. (C and D) WNV_{KUN}-infected cells were pre-treated with control siRNA. (E and F) Cells were treated with RTN3.1A-specific siRNA and infected with WNV_{KUN}. All scale bars represent 500 nm. Nu, nucleus; M, mitochondria; ER, endoplasmic reticulum; Ve, virus-induced replication vesicles; CM/PC, convoluted membranes/paracrystalline arrays; VP, vesicle packets; vi, virus particles.

(G) Quantitation of the area/size of the CM/PC (μm^2) structures observed in the different sample groups (**$p < 0.02$ as measured by Student's t test) and error bars indicate mean ± SD.

(H) Quantitation of replication vesicles per infected cell in EM thin sections (2D only) (****$p < 0.0001$ as measured by Student's t test) and error bars indicate mean ± SD.

See also Figure S1.

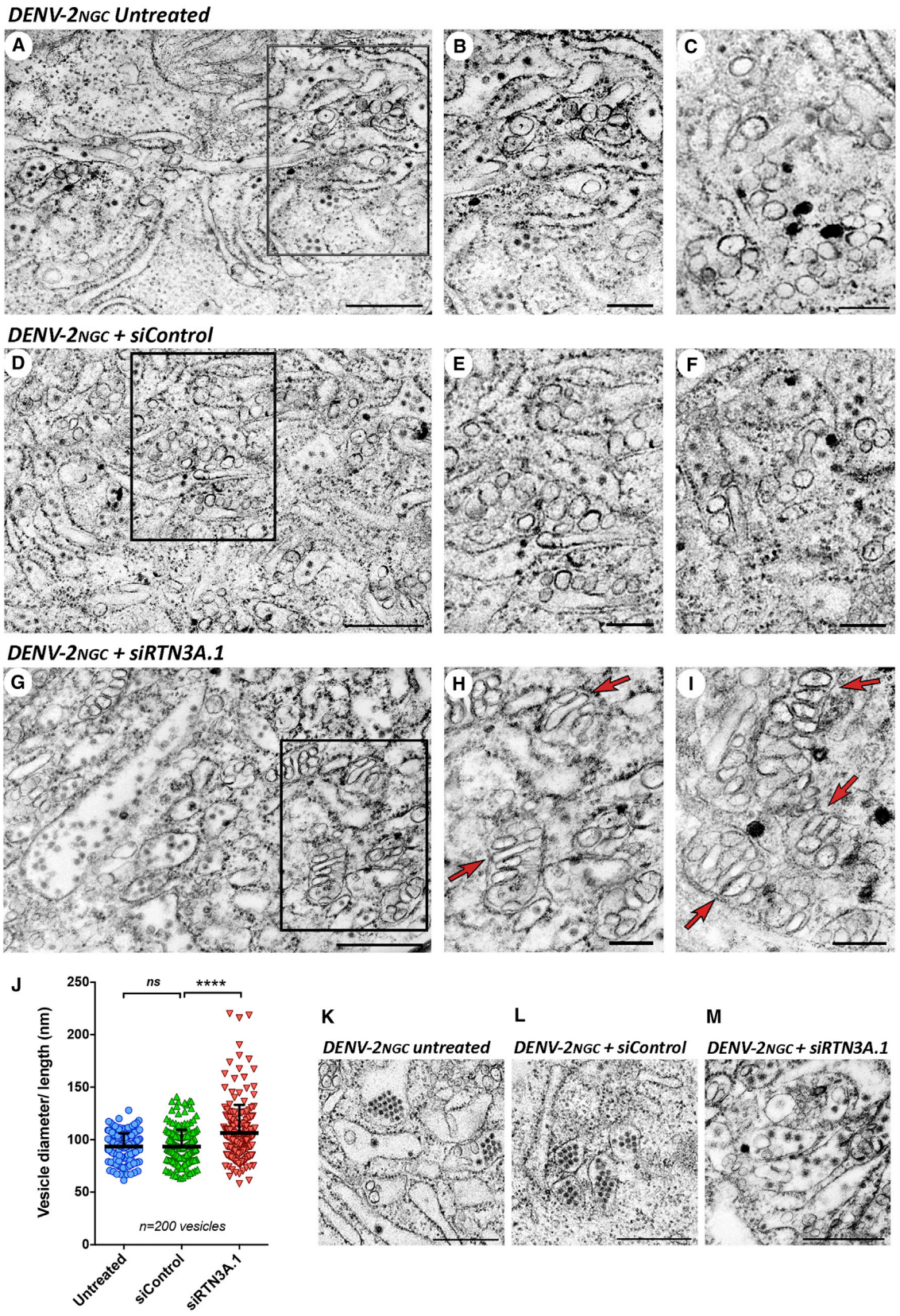

(legend on next page)

Furthermore, to determine if in fact WNV_{KUN} NS4A(−2K) was interacting with RTN3.1A, we performed fluorescence resonance energy transfer (FRET) analysis. For FRET to occur, we used NS4A-tagged GFP as the energy donor and RTN3.1A-tagged mCherry as the energy acceptor, which would undergo FRET if these two proteins were less than 5.24 nm apart (Patterson et al., 2000). We observed negligible FRET signal during co-transfection of cells with the WNV_{KUN} NS4B-GFP, DENV-2_{NGC}, and $ZIKV_{AFR}$ GFP-NS4A(−2K) with RTN3.1A-mCherry (Figures 7B and 7C), indicating that these proteins were not interacting. However, upon co-transfection of WNV_{KUN} GFP-NS4A(−2K) with RTN3.1A-mCherry, a robust increase in FRET signal was observed in comparison to NS4B-GFP. These results suggest that only WNV_{KUN} GFP-NS4A(−2K) interacts with RTN3.1A-mCherry, although we cannot completely exclude an intermediate interaction partner.

WNV_{KUN} NS4A Associates and Co-localizes with RTN3.1A via Its Most N-terminal TM Domain

As we determined that RTN3.1A specifically co-localizes and interacts with the WNV_{KUN} GFP-NS4A(−2K) protein, we aimed to identify a potential domain within NS4A that mediates protein-protein interaction. To investigate this, we utilized our existing GFP, WNV_{KUN} NS4B-GFP, and GFP-NS4A expression constructs that had sequential C-terminal hydrophobic domain deletions (Ambrose and Mackenzie, 2011b) in combination with recombinant mCherry-tagged RTN3.1A. These constructs were transfected into HeLa cells for analysis via FRET (Figures 7D and 7E) and into HEK293T cells for coimmunoprecipitation (coIP) experiments (Figure 7F).

Upon co-transfection with GFP-NS4A, GFP-NS4A(−2K), GFP-NS4A(-TM2), or GFP-NS4A(-TM1) with RTN3.1A-mCherry, a robust FRET signal was observed. Interestingly, removal of the last TM domain significantly reduced FRET efficiency (Figures 7D and 7E). These observations suggest that the interaction between NS4A and RTN3.1A is mediated via the first N-terminal hydrophobic domain of NS4A and that these two proteins interact at a distance less than or equal to 5.24 nm.

To support an association between NS4A and RTN3.1A, we performed immunoprecipitation experiments with the *cmyc-HIS*-tagged RTN3.1A and the GFP-NS4A recombinant proteins (Figure 7F). We observed that only minor amounts of GFP-NS4A, GFP-NS4A(−2K), and GFP-NS4A(TM0) of the recombinant forms of GFP-NS4A were co-purified with *cmyc-HIS*-RTN3.1A (Figure 7F). In contrast, we observed that GFP-NS4A(TM2) and GFP-NS4A(TM1) were predominately co-purified with *cmyc-HIS*-RTN3.1A (Figure 7F). This observation is in agreement with the FRET analysis (Figures 7D and 7E). These results may also indicate that, although both proximal to each other within the ER, the presence of the 2K peptide (not normally present on the mature NS4A protein) may hinder the interaction with RTN3.1A. We also cannot discount any subtle differences in the protein conformation between mCherry- and *cmyc-HIS*-tagged RTN3.1A that could contribute to these observations.

Overall, we have shown that the host protein RTN3.1A interacts with the WNV_{KUN} viral protein NS4A, potentially via the TM domains at the N terminus of NS4A. We believe this interaction aids in stabilizing the NS4A protein to facilitate the membrane-bending and -remodelling capabilities of both RTN3.1A and NS4A to promote the induction of ER membranes characteristic of flavivirus infection.

DISCUSSION

Due to their limited genome capacity, (+) sense RNA viruses work in sync with host factors (both protein and lipid) to create unique microenvironments for replication. The host ER-bound RTN proteins are present in all eukaryotic organisms, with multiple introns and exons giving rise to numerous isoforms; however, they all share a common RHD (Yang and Strittmatter, 2007). In this study, we have shown that the host ER-shaping protein RTN3.1A contributes to the replication cycle of WNV_{KUN}, DENV-2_{NGC}, and $ZIKV_{AFR}$ and that, in the absence of RTN3.1A, the viral ER proteins NS4B and NS4A are susceptible to degradation via the host proteasome. Furthermore, we have demonstrated that RTN3.1A potentially interacts with the WNV_{KUN} NS4A protein to aid in the remodelling of the ER membrane to facilitate efficient virus replication.

The RTN protein family has differential effects in regulating viral replication. Members of the *Picornaviridae* family of viruses initially replicate on positively curved single-membrane vesicles; however, as infection progresses, these structures become double-membrane vesicles protruding out to the cytoplasm from the ER (Bienz et al., 1983; Schlegel et al., 1996; Limpens et al., 2011; Belov et al., 2012). Tang et al. (2007) observed that EV71 2C protein and dsRNA localized with RTN3.1A by IF and silencing of RTN3.1A reduced EV71 dsRNA and protein levels. Furthermore, replication of BMV occurs on negatively curved (protruding into the ER lumen) ER membranes (termed spherules) that are induced by the BMV 1a protein (Schwartz et al., 2002). Deletion of the RTN1, 2 and Yop1 in yeast prevented BMV 1a to induce spherules and recruit viral RNA, inhibiting replication by 80%–90% (Diaz et al., 2010). The only report for a member of the *Flaviviridae* family of viruses has

Figure 4. RTN3.1A Silencing Elongates Virus-Induced Replication Vesicles of the ER during DENV-2_{NGC} Replication

(A–I) HEK293T cells were untreated (A–C) or treated with control siRNA (D–F) or siRNA specific for the host *RTN3.1A* gene (G–I) prior to DENV-2_{NGC} infection. Cells were harvested 48 h.p.i. and processed for EM analysis. (A–C) Untreated DENV-2_{NGC} infected cells are shown. Inset of (A) is magnified in (B). (D–F) DENV-2_{NGC}-infected cells were pre-treated with control siRNA. Inset of (D) is magnified in (E). (G–I) Cells were treated with RTN3.1A-specific siRNA and infected with DENV-2_{NGC}. Inset of (G) is magnified in (H). Scale bars represent 500 nm (A, D, and G) or 200 nm (B, C, E, F, H, and I). In all cases arrows indicate elongated vesicles. (J) Quantitation of the replication vesicle diameter/length (nm) among all samples (n = 200 vesicles; ****$p < 0.0001$ as measured by Student's t test) and error bars indicate mean ± SD.

(K–M) Typical DENV-2_{NGC} virus stacks in untreated (K) and control siRNA-treated cell preparations (L) in contrast to predominantly fuzzy-appearing virus particles in RTN3.1A-silenced cells (M). Scale bars represent 500 nm.

See also Figure S1.

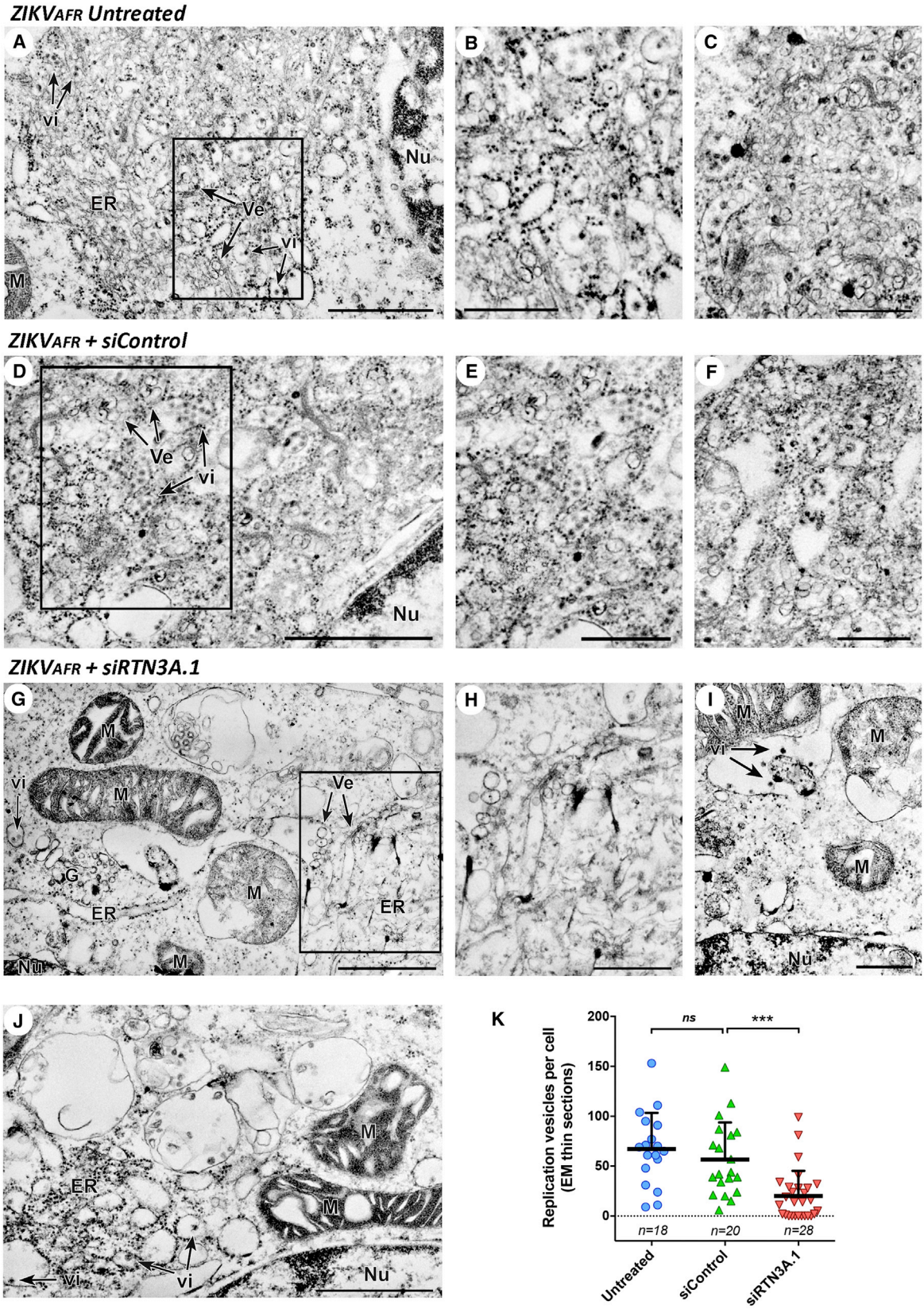

(legend on next page)

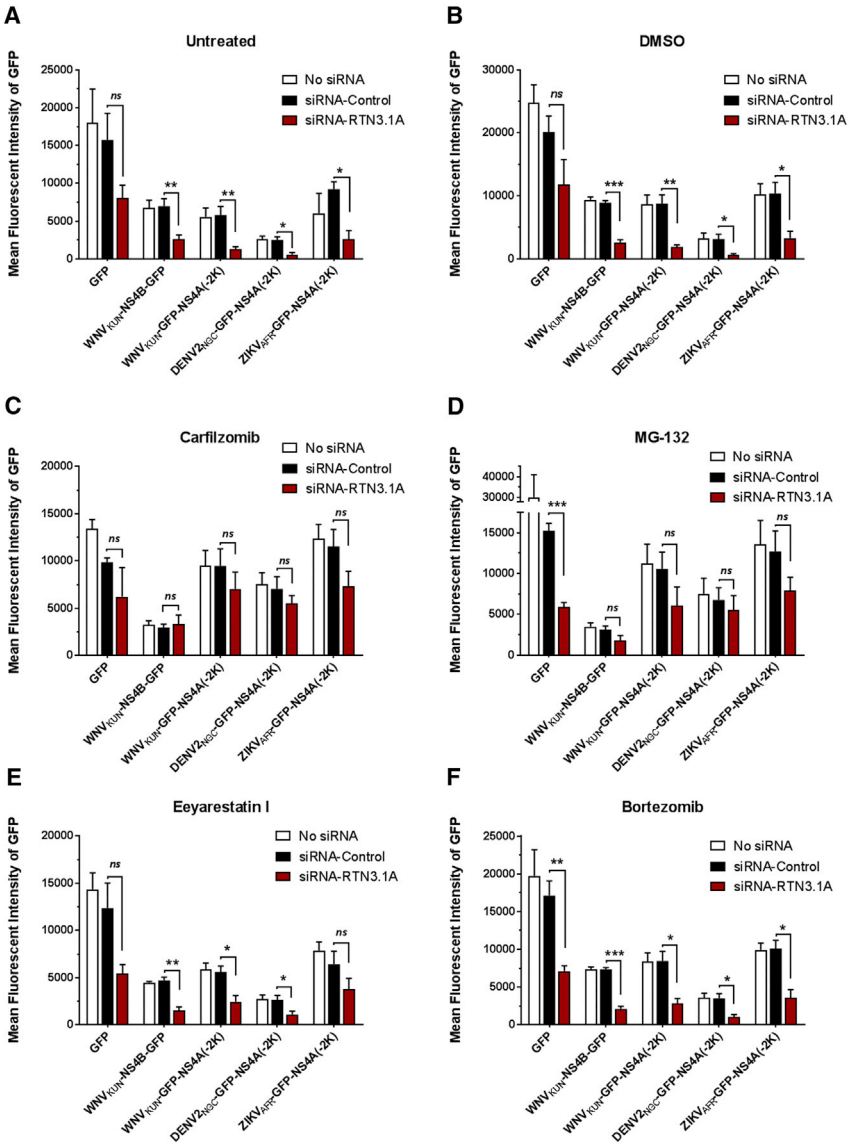

Figure 6. Viral ER Protein Degradation Is Partially Rescued via Proteasome Inhibition

(A–F) HEK293T cells were untreated or treated with control siRNA or siRNA specific for the host *RTN3.1A* gene; transfected with cDNA plasmids encoding GFP, WNV_{KUN} NS4B-GFP, WNV_{KUN} GFP-NS4A(−2K), DENV-2_{NGC} GFP-NS4A(−2K), or $ZIKV_{AFR}$ GFP-NS4A(−2K) constructs; and untreated (A) or treated with 0.1% DMSO (B, n = 3), carfilzomib (C, 0.5 μM) (n = 3), MG-132 (D, 0.5 μM) (n = 3), eeyarestatin I (E, 10 μM) (n = 3), or bortezomib (F, 10 nM) (n = 3). At 20 hr post-treatment, cells were fixed for flow cytometry and mean fluorescence intensity is plotted in graphical form. Error bars indicate ± SEM of replicate analysis of replicate experiments, and significance was assessed by Student's t test (GraphPad Prism 6).

shown that RTN3.1A may act as an anti-viral mediator during HCV replication (Barajas et al., 2014). The authors showed that RTN3.1A binds to NS4B, prevents its self-dimerization, and thus inhibits replication (Barajas et al., 2014). The above study implies that HCV NS4B can associate with and proliferate the HCV membranous web independently of RTN3.1A (Barajas et al., 2014).

During flavivirus replication, two important structures protruding the ER have been characterized. First, the formation of VPs, which house the viral RC, and, second, the CM/PC structures, where viral translation is proposed to occur (Westaway et al., 1997). The exact mechanisms underlying the formation of these membranous microenvironments remain uncharacterized; however, these structures are required for efficient flavivirus replication. During this study, we observed that RTN3.1A contributes significantly to the biogenesis and structure of the VP for WNV_{KUN}, DENV-2_{NGC}, and $ZIKV_{AFR}$ and the CM/PC for WNV_{KUN} infection. Interestingly, the silencing of RTN3.1A expression attenuated viral RNA levels during DENV-2_{NGC} and $ZIKV_{AFR}$ infection (Figure 2A, ii and iii); however, this suppression did not significantly impair WNV_{KUN} RNA levels (Figure 2A, i). However, the reduced expression of RTN3.1A significantly impaired viral protein translation and the production of infectious viral particles for all viruses (Figure 2). Importantly, the silencing of RTN3.1A had a dramatic effect on the ability and capacity of each of the flaviviruses to remodel intracellular membranes (Figures 3, 4, and 5). We observed that silencing of RTN3.1A during WNV_{KUN} infection dramatically reduced the size and area of the CM/PC and prompted a decrease

Figure 5. RTN3A Silencing during $ZIKV_{AFR}$ Infection Impairs Virus-Induced Vesicle Formation

(A–J) HEK293T cells were untreated (A–C) or treated with control siRNA (D–F) or siRNA specific for the host *RTN3.1A* gene (G–J) prior to $ZIKV_{AFR}$ infection. Cells were harvested 36 h.p.i. and subject to EM analysis. (A–C) Untreated $ZIKV_{AFR}$-infected cells are shown. Inset of (A) is magnified in (B). (D–F) Cells were pre-treated with control siRNA and infected with $ZIKV_{AFR}$. Inset of (D) is magnified in (E). (G–J) RTN3.1A-silenced $ZIKV_{AFR}$-infected cells are shown. Inset of (G) is magnified in (H). Scale bars represent 500 nm. Nu, nucleus; M, mitochondria; ER, endoplasmic reticulum; G, Golgi;Ve, virus-induced vesicles in the ER; vi, virus particles.

(K) Quantitation of replication vesicle numbers per infected cell in EM thin sections (2D only) (****$p < 0.0001$ as measured by Student's t test) and error bars indicate mean ± SD.

See also Figure S1.

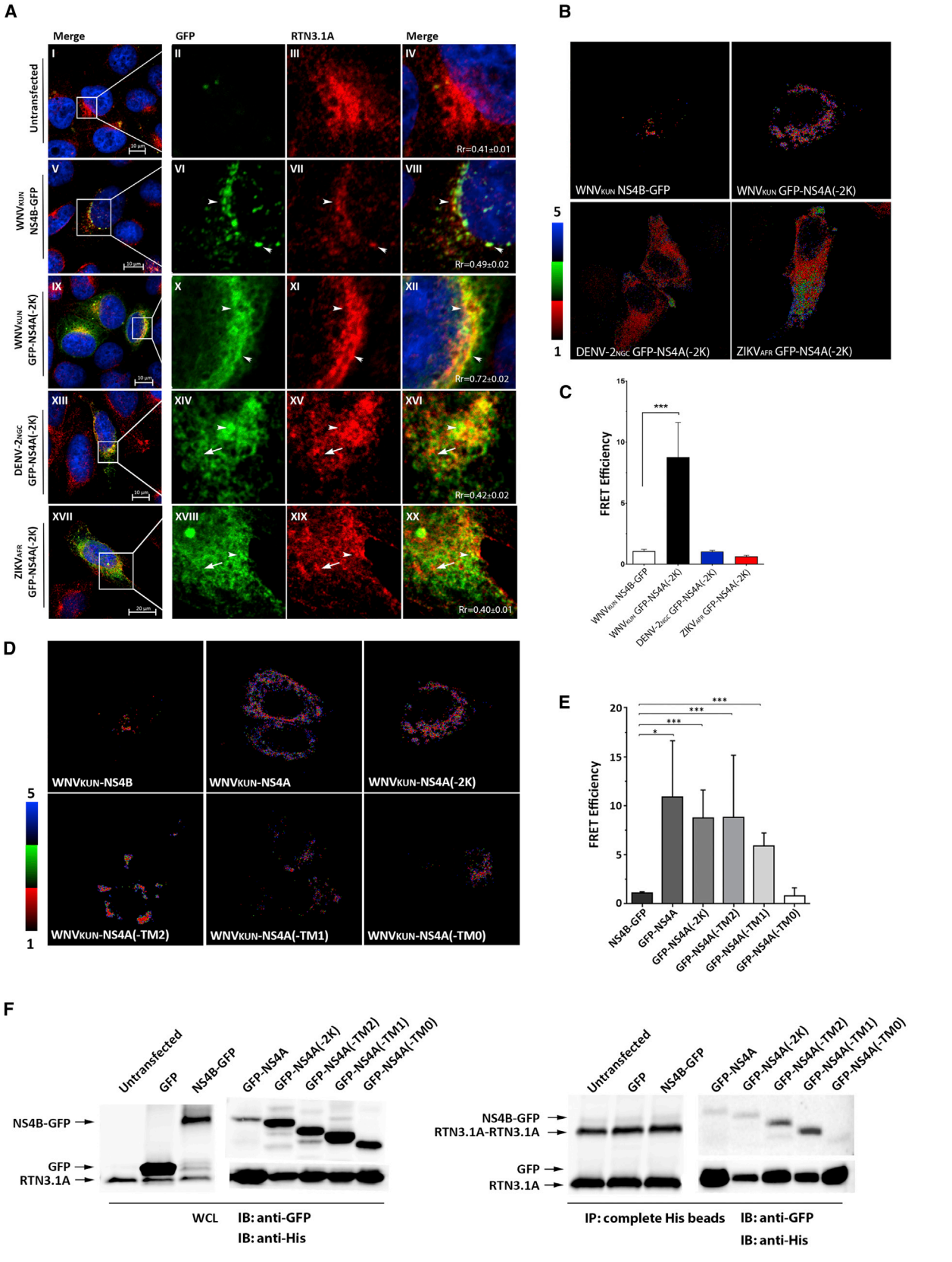

(legend on next page)

in replication vesicle number, whereas, for DENV-2_{NGC} and $ZIKV_{AFR}$, there were perturbations in vesicle morphology, length, and number, respectively, all of which contributed to decreased replication, viral production, and secretion of infectious virus. It is well accepted that the induction of the characteristic flavivirus membranous structures contributes to efficient virus replication, but here we provide evidence that WNV_{KUN}, DENV-2_{NGC}, and $ZIKV_{AFR}$ may utilize the same host factor to enable the biogenesis of these membranes, although each virus does it in a subtly unique manner.

The flavivirus genome contains a single open reading frame (ORF) where an approximate 1:1 ratio of viral proteins is translated. Interestingly, our results have demonstrated that suppression of RTN3.1A resulted in an enhanced reduction in NS4A proteins levels compared to NS1 and NS5 levels during WNV_{KUN} and DENV-2_{NGC} replication (Figure 2B, i–iii). This was further confirmed by a reduction in transient expression of recombinant NS4A-GFP expression during RTN3.1A silencing (Figure 6A). This suggests that, in the absence of RTN3.1A, flavivirus NS4A is destabilized and thus prone to degradation, possibly via the proteasome. Previously, reports from our group have demonstrated an increase in ER-associated degradation of WNV_{KUN} NS4A harboring point mutations within conserved regions. We observed that NS4A levels are restored when mutant NS4A-infected cells were treated with the proteasome inhibitor bortezomib, which acts on the 20S subunit of the 26S proteasome (Ambrose and Mackenzie, 2015). However, we were unable to prevent NS4A degradation during RTN3.1A suppression with the proteasome inhibitor bortezomib (Figure 6F), but we were able to do so with carfilzomib and MG132, which both act on the 20S subunit of the 26S proteasome (Wang et al., 2013; Pautasso et al., 2013; Goldberg, 2012). In contrast, eeyarestatin I, targeting the 19S subunit of the 26S proteasome, did not rescue expression. Thus, our results demonstrated that blocking the 20S subunit rather than the 19S subunit partially rescued viral protein expression levels (Figures 6C, 6D, and 6F, respectively).

These observations suggest that RTN3.1A may interact with NS4A within the ER membrane, thus protecting NS4A from subsequent ER-associated degradation. One possible explanation is that RTN3.1A aids in the oligomerization of NS4A, as some recent reports have indicated that the oligomerization of DENV-2_{NGC} NS4A is mediated via the first TM domain (Lee et al., 2015; Stern et al., 2013), the domain potentially responsible for RTN3.1A-NS4A interaction. We are currently exploring this possibility. The flavivirus NS4A protein is a highly conserved protein with multiple membrane-spanning domains (Miller et al., 2007; Roosendaal et al., 2006) (Figure S2). Intriguingly, mutations that affect the cleavage between NS4A and 2K in the WNV_{KUN} infectious clone resulted in the accumulation of full-length NS4A that was lethal to virus infection (Ambrose and Mackenzie, 2011a). We also observed that the full-length NS4A bound less strongly to RTN3.1A (Figure 7), suggesting that 2K may invoke a steric hindrance to the NS4A-RTN3.1A interaction. This would suggest that efficient cleavage of NS4A from 2K promotes an association of RTN3.1A with the TM regions within the N terminus to stabilize and potentially promote oligomerization of NS4A and operate in concert to facilitate membrane remodelling.

NS4A is a multifunctional protein, and previous studies have shown that NS4A facilitates replication of a number of flaviviruses (Lindenbach and Rice, 1999; Li et al., 2015; Zou et al., 2015); DENV-2_{NGC} NS4A interacts with scaffolding protein vimentin (Teo and Chu, 2014); DENV-2 NS4A N terminus preferentially binds to highly curved membranes (Hung et al., 2015a, 2015b); WNV_{KUN} NS4A regulates the unfolded protein response (Ambrose and Mackenzie, 2011b); flavivirus NS4A regulates interferon signaling and innate immune responses (Liu et al., 2005; Muñoz-Jordan et al., 2003; Dalrymple et al., 2015; He et al., 2016) and induces autophagy (McLean et al., 2011; Liang et al., 2016; Blázquez et al., 2015); and now we have demonstrated that NS4A interacts with RTN3.1A to aid in replication, possibly via its ER membrane-bending capacity during replication complex formation.

Overall this study has contributed to the understanding of host components during the replication cycles of the flaviviruses WNV_{KUN}, DENV-2_{NGC}, and $ZIKV_{AFR}$ and the role of host RTN3.1A protein to the replication of a growing number of (+) sense RNA viruses. Our results suggest that RTN3.1A is crucial for efficient viral replication and contributes to the membrane remodelling observed during flavivirus infection by interacting with the WNV_{KUN} NS4A protein to promote increased stability and aid in the function of NS4A. The possibility exists that targeting host factors, which aid in virally induced membrane structures for antiviral development, could reduce the impact of flavivirus infection and, thus, disease proliferation.

Figure 7. RTN3.1A Co-localizes and Interacts Solely with the WNV_{KUN} NS4A(−2K) via the N-terminal TM Domain, but Not DENV-2_{NGC} and $ZIKV_{AFR}$ NS4A(−2K)

(A) HeLa cells were mock transfected (I–IV) or transfected with cDNA plasmids encoding WNV_{KUN} NS4B-GFP (V–VIII), WNV_{KUN} GFP-NS4A(−2K) (IX–XII), DENV-2_{NGC} GFP-NS4A(−2K) (XIII–XVI), or $ZIKV_{AFR}$ GFP-NS4A(−2K) (XVII–XX), and 24 hr later immunolabeled with antibodies against endogenous RTN3.1A (III, VII, XI, XV, and XIX; red). The merged images are provided at both low (I, V, IX, XIII, and XVII) and high (IV, VIII, XII, XVI, and XX) magnification, with a yellow hue indicating regions of co-localization. Arrowheads indicate regions of high co-incidental staining and arrows indicate regions where co-localization is not observed. Pearson's coefficient (co-localization; *Rr*) was determined by the JaCOP plugin software in ImageJ on multiple images collected over replicate experiments (*Rr* values in IV, VIII, XII, XVI, and XX). Error bars indicate mean *Rr* ± SEM, and significance was determined by Student's t test (GraphPad Prism 6).
(B and D) HeLa cells were co-transfected with cDNA plasmids encoding RTN3.1A-mCherry and WNV_{KUN} NS4B-GFP, WNV_{KUN} GFP-NS4A(−2K), DENV-2_{NGC} GFP-NS4A(−2K), or $ZIKV_{AFR}$ GFP-NS4A(−2K) constructs (B) or WNV_{KUN} NS4B-GFP, GFP-NS4A, GFP-NS4A(−2K), GFP-NS4A(-TM2), GFP-NS4A(-TM1), or GFP-NS4A(-TM0) constructs (D) and assessed via FRET. Blue hue represents areas of high FRET while red hue represents areas of low FRET.
(C and E) FRET efficiency depicted in (B) and (D), respectively, was calculated by the Leica LAS software. Error bars indicate ± SEM of replicate analysis of replicate experiments (n = 4), and significance was assessed by Student's t test (GraphPad Prism 6).
(F) HEK293T cells were co-transfected with cDNA plasmids encoding recombinant GFP, WNV_{KUN} NS4B-GFP, GFP-NS4A, GFP-NS4A(−2K), GFP-NS4A(-TM2), GFP-NS4A(-TM1), or GFP-NS4A(-TM0) constructs or cMyc-HIS-RTN3.1A. At 24 hr post-transfection, whole-cell lysates were collected and analyzed by western blotting for expression of the recombinant proteins or after cOmplete HIS-Tag Resin purification precipitation with antibodies raised against RTN3.1A and GFP.

EXPERIMENTAL PROCEDURES

Cell Culture and Viral Infection

HeLa and HEK293T cells were maintained in DMEM (Life Technologies) supplemented with 5% fetal calf serum (FCS; Thermo Fisher Scientific) and 200 mM GlutaMAX (Glx; Gibco). Cells were grown at 37°C with 5% CO_2. WNV_{KUN} stocks were propagated from a WNV_{KUN} MRM61C secondary stock in Vero C1008 cells at 37°C and 5% CO_2 in DMEM supplemented with 0.2% (w/v) BSA (Sigma-Aldrich) for 48 hr. DENV-2_{NGC} was kindly provided by David Jans (Monash University) and propagated in *Aedes albopictus* C6/36 cells at 28°C in DMEM for 5 days. $ZIKV_{AFR}$ was kindly provided by Julian Druce (VIDRL, Melbourne) and propagated in *Aedes albopictus* C6/36 cells at 28°C in DMEM for 4 days.

IF Analysis

HeLa cells were infected with WNV_{KUN}, DENV-2_{NGC}, or $ZIKV_{AFR}$ or transfected with appropriate constructs. Cells were fixed for IF analysis as previously described (Aktepe et al., 2015). Cells were visualized on the Zeiss confocal microscope (LSM 710), and figures were assembled using Adobe Photoshop. All images were taken under identical acquisition settings, and multiple images were collected from triplicate experiments for analysis. Co-localization was determined by Pearson's coefficient (Bolte and Cordelières, 2006) using the ImageJ JACoP plugin software. A co-efficient value exceeding 0.50 was considered as co-localization.

FRET

HeLa cells were co-transfected with GFP-NS4B, GFP-NS4A, GFP-NS4A(−2K), GFP-NS4A(-TM2), GFP-NS4A(-TM1), and GFP-NS4A(-TM0) as FRET donor and RTN3.1A-mCherry as FRET acceptor. At 20 hr post-transfection, cells were fixed with 4% paraformaldehyde (PFA) for 15 min, followed by 0.2 M glycine treatment. Coverslips were mounted using Ultramount. Leica SP5 microscope equipped with FRET-sensitized emission was used for FRET analysis.

RTN3.1A Knockdown

HEK293T cells were reverse transfected with 0.25 μM siRNA (Bioneer) and RNAiMAX (Invitrogen) in opti-MEM (Gibco). Cells were incubated at 37°C and 5% CO_2 for 24 hr. Cells were once again transfected with 0.5 μM siRNA. At 4, 14, and 24 hr post-transfection, cells were infected with DENV-2_{NCG}, $ZIKV_{AFR}$, and WNV_{KUN} and incubated for a further 42, 32, and 22 hr, respectively.

RNA Extraction and qRT-PCR

RNA was extracted from cells with Trizol Reagent (Life Technologies) by following the manufacturer's protocol. SuperScript III Reverse Transcriptase (Invitrogen) and strand-specific primers for WNV_{KUN}, DENV-2_{NGC}, and $ZIKV_{AFR}$ were used to generate cDNA for viral positive and negative sense RNA, and GAPDH was used as the internal control. qRT-PCR was performed with ITaq Universal SybrGreen (Bio-Rad), 10-μM forward and reverse primers, and various templates.

Western Blot Analysis

Western blot analysis was performed as previously described (Aktepe et al., 2015). Briefly, infected cells were lysed with NP-40 lysis buffer containing protease inhibitors and loaded on a Bis/Tris polyacrylamide gel. Proteins were transferred to a Hi-Bond enhanced chemiluminescence (ECL) nitrocellulose membrane and incubated with primary antibodies overnight at 4°C. Membranes were incubated with species-specific secondary antibodies conjugated to either Alexa Fluor 488 or 647, and proteins were detected with the Bio-Rad Pharos FX system.

cOmplete HIS-Tag Resin Purification

cOmplete HIS-Tag Resin (Roche) was used to purify HIS-tagged proteins. Resin was washed twice with NP-40 buffer, added to lysate, and incubated overnight on the orbital rotator at 4°C. The following day, samples were centrifuged and washed 3 times for 10 min at 4°C with relaxed wash buffer (150 mM NaCl, 2 mM $MgCl_2$, 10 mM imidazole, and 50 mM Tris [pH 8.0]; just prior to use, adding 1/500 protease inhibitor cocktail), followed by 3 washes with stringent wash buffer (150 mM NaCl, 2 mM $MgCl_2$, 30 mM imidazole, and 50 mM Tris [pH 8.0]; just prior to use, adding 1/500 protease inhibitor cocktail). The target protein was eluted with 40 μL elution buffer (150 mM NaCl, 2 mM $MgCl_2$, 300 mM imidazole, 50 mM Tris [pH 8.0] and prior to use 1/500 protease inhibitor cocktail) by incubating at 50°C for 10 min. Supernatant was transferred to a new microcentrifuge tube and stored at −80°C until required.

Plaque Assay and Foci-Forming Unit Assay

Tissue culture fluid was collected from siRNA-treated and/or WNV_{KUN}-, DENV-2_{NGC}-, or $ZIKV_{AFR}$-infected cells, and infectious virus particles were determined by plaque assay or foci-forming assay for WNV_{KUN}, $ZIKV_{AFR}$, and DENV-2_{NGC}, respectively, as previously described (Aktepe et al., 2015).

Drug Treatment for Proteasome Inhibition

Following knockdown of RTN3.1A, HEK293T cells were transfected with GFP, WNV_{KUN} NS4B-GFP, WNV_{KUN}, DENV-2_{NGC}, and $ZIKV_{AFR}$ GFP-NS4A(−2K). At 4 hr post-transfection, cells were untreated or treated with carfilzomib (0.5 μM), MG-132 (0.5 μM), eeyarestatin I (10 μM), bortezomib (10 nM), and DMSO as a solvent control (0.1% DMSO). At 20 hr post-treatment; cells were fixed and analyzed by flow cytometry.

Flow Cytometry

Following proteasome inhibition, cells were fixed (2% PFA in PBS), permeabilized (0.1% Triton-X and 1% FCS in PBS), and labeled for RTN3.1A in staining buffer (5% FCS and 0.1% sodium azide in PBS). Samples were washed and incubated with species-specific secondary antibody, then washed and resuspended in PBS for flow cytometry analysis. Cell profiles were determined by flow cytometry using a BD LSR Fortessa flow cytometer, and data were analyzed using FlowJo software (Tree Star).

Resin Embedding and Thin Sectioning for EM

Infected cells were fixed and processed for EM as previously described (Westaway et al., 1997). Thin sections (60 nm) were cut on a Leica UC7 ultramicrotome using a Diatome diamond knife, contrasted with 2% aqueous uranyl acetate (UA) and Reynold's lead citrate before viewing in a Technai F20 or F30 transmission electron microscope. The size/area of WNV_{KUN}-induced CM/PC was measured in reference to individual scale bars in multiple EM images using ImageJ software. Likewise, the diameter/length of Dengue-induced vesicles was measured using the ruler tool in Photoshop CS6 and referenced to scale bars. WNV_{KUN}, DENV-2_{NGC}, and $ZIKV_{AFR}$ datasets were graphed, and unpaired t tests were performed using GraphPad Prism 6.

Statistics

Unless specified otherwise, an unpaired Student's t test was performed using GraphPad Prism 6 to test for statistical significance. Error bars indicate mean ± SEM or SD, and "n" represents independent experimental replicates, number of cells, number of replication vesicles (VPs), or area of CM/PC per cell (exact numbers are specified in results and figure legends). The p values are indicated by *$p < 0.05$, **$p < 0.01$, ***$p < 0.001$, and ****$p < 0.0001$.

SUPPLEMENTAL INFORMATION

Supplemental Information includes Supplemental Experimental Procedures and two figures and can be found with this article online at https://doi.org/10.1016/j.celrep.2017.10.055.

AUTHOR CONTRIBUTIONS

Conceptualization, T.E.A., J.M.M., and S.L.; Methodology, T.E.A., J.M.M., S.L., and J.E.P.; Investigation, T.E.A., S.L., and J.E.P.; Resources, J.M.M. and C.P.S.; Writing – Original Draft, T.E.A., and S.L.; Writing – Review and Editing, T.E.A., J.M.M., and S.L.; Visualization, T.E.A., S.L., J.M.M., and J.E.P.; Supervision, J.M.M., S.L., and C.P.S.; Project Administration, T.E.A. and J.M.M.; Funding Acquisition, J.M.M.

ACKNOWLEDGMENTS

We thank the Bio21 Institutes' Electron Microscopy Unit for their equipment and the expertise of Eric Hanssen, Zlatan Trifunovic, and Sergey Rubanov. We also thank Alexander Khromykh, Roy Hall, and Paul Young for generously providing the WNV and DENV antibodies; Julian Druce for providing $ZIKV_{AFR}$; David Jans for providing DENV-2_{NGC} and DENV antibodies; Daniel Watterson (University of Queensland) for advice with the DENV foci-forming assay; and Paulina Koszalka (University of Melbourne, Peter Doherty Institute for Infection and Immunity) for advice and aid with the cloning on DENV-2_{NGC} and $ZIKV_{AFR}$ GFP-NS4A constructs. This research was supported by project grants (1004619 and 1081786) to J.M.M. from the National Health and Medical Research Council of Australia.

Received: March 10, 2017
Revised: September 24, 2017
Accepted: October 12, 2017
Published: November 7, 2017

REFERENCES

Ahlquist, P., Noueiry, A.O., Lee, W.-M., Kushner, D.B., and Dye, B.T. (2003). Host factors in positive-strand RNA virus genome replication. J. Virol. *77*, 8181–8186.

Aktepe, T.E., Pham, H., and Mackenzie, J.M. (2015). Differential utilisation of ceramide during replication of the flaviviruses West Nile and dengue virus. Virology *484*, 241–250.

Ambrose, R.L., and Mackenzie, J.M. (2011a). A conserved peptide in West Nile virus NS4A protein contributes to proteolytic processing and is essential for replication. J. Virol. *85*, 11274–11282.

Ambrose, R.L., and Mackenzie, J.M. (2011b). West Nile virus differentially modulates the unfolded protein response to facilitate replication and immune evasion. J. Virol. *85*, 2723–2732.

Ambrose, R.L., and Mackenzie, J.M. (2015). Conserved amino acids within the N-terminus of the West Nile virus NS4A protein contribute to virus replication, protein stability and membrane proliferation. Virology *481*, 95–106.

Barajas, D., Xu, K., Sharma, M., Wu, C.-Y., and Nagy, P.D. (2014). Tombusviruses upregulate phospholipid biosynthesis via interaction between p33 replication protein and yeast lipid sensor proteins during virus replication in yeast. Virology *471-473*, 72–80.

Belov, G.A., Nair, V., Hansen, B.T., Hoyt, F.H., Fischer, E.R., and Ehrenfeld, E. (2012). Complex dynamic development of poliovirus membranous replication complexes. J. Virol. *86*, 302–312.

Bienz, K., Egger, D., Rasser, Y., and Bossart, W. (1983). Intracellular distribution of poliovirus proteins and the induction of virus-specific cytoplasmic structures. Virology *131*, 39–48.

Blázquez, A.B., Martín-Acebes, M.A., and Saiz, J.C. (2015). Amino acid substitutions in the non-structural proteins 4A or 4B modulate the induction of autophagy in West Nile virus infected cells independently of the activation of the unfolded protein response. Front. Microbiol. *5*, 797.

Bolte, S., and Cordelières, F.P. (2006). A guided tour into subcellular colocalization analysis in light microscopy. J. Microsc. *224*, 213–232.

Cortese, M., Goellner, S., Acosta, E.G., Neufeldt, C.J., Oleksiuk, O., Lampe, M., Haselmann, U., Funaya, C., Schieber, N., Ronchi, P., et al. (2017). Ultrastructural Characterization of Zika Virus Replication Factories. Cell Rep. *18*, 2113–2123.

Dalrymple, N.A., Cimica, V., and Mackow, E.R. (2015). Dengue Virus NS Proteins Inhibit RIG-I/MAVS Signaling by Blocking TBK1/IRF3 Phosphorylation: Dengue Virus Serotype 1 NS4A Is a Unique Interferon-Regulating Virulence Determinant. MBio *6*, e00553–15.

Diaz, A., Wang, X., and Ahlquist, P. (2010). Membrane-shaping host reticulon proteins play crucial roles in viral RNA replication compartment formation and function. Proc. Natl. Acad. Sci. USA *107*, 16291–16296.

Gillespie, L.K., Hoenen, A., Morgan, G., and Mackenzie, J.M. (2010). The endoplasmic reticulum provides the membrane platform for biogenesis of the flavivirus replication complex. J. Virol. *84*, 10438–10447.

Goldberg, A.L. (2012). Development of proteasome inhibitors as research tools and cancer drugs (Rockefeller University Press).

He, Z., Zhu, X., Wen, W., Yuan, J., Hu, Y., Chen, J., An, S., Dong, X., Lin, C., Yu, J., et al. (2016). Dengue Virus Subverts Host Innate Immunity by Targeting Adaptor Protein MAVS. J. Virol. *90*, 7219–7230.

Hoenen, A., Liu, W., Kochs, G., Khromykh, A.A., and Mackenzie, J.M. (2007). West Nile virus-induced cytoplasmic membrane structures provide partial protection against the interferon-induced antiviral MxA protein. J. Gen. Virol. *88*, 3013–3017.

Hoenen, A., Gillespie, L., Morgan, G., van der Heide, P., Khromykh, A., and Mackenzie, J. (2014). The West Nile virus assembly process evades the conserved antiviral mechanism of the interferon-induced MxA protein. Virology *448*, 104–116.

Hung, Y.F., Schwarten, M., Hoffmann, S., Willbold, D., Sklan, E.H., and Koenig, B. (2015a). Amino Terminal Region of Dengue Virus NS4A Cytosolic Domain Binds to Highly Curved Liposomes. Viruses *7*, 4119–4130.

Hung, Y.F., Schwarten, M., Schünke, S., Thiagarajan-Rosenkranz, P., Hoffmann, S., Sklan, E.H., Willbold, D., and Koenig, B.W. (2015b). Dengue virus NS4A cytoplasmic domain binding to liposomes is sensitive to membrane curvature. Biochim. Biophys. Acta *1848*, 1119–1126.

Junjhon, J., Pennington, J.G., Edwards, T.J., Perera, R., Lanman, J., and Kuhn, R.J. (2014). Ultrastructural characterization and three-dimensional architecture of replication sites in dengue virus-infected mosquito cells. J. Virol. *88*, 4687–4697.

Kume, H., Konishi, Y., Murayama, K.S., Kametani, F., and Araki, W. (2009). Expression of reticulon 3 in Alzheimer's disease brain. Neuropathol. Appl. Neurobiol. *35*, 178–188.

Lee, C.M., Xie, X., Zou, J., Li, S.-H., Lee, M.Y.Q., Dong, H., Qin, C.-F., Kang, C., and Shi, P.-Y. (2015). Determinants of Dengue Virus NS4A Protein Oligomerization. J. Virol. *89*, 6171–6183.

Li, X.D., Ye, H.Q., Deng, C.L., Liu, S.Q., Zhang, H.L., Shang, B.D., Shi, P.Y., Yuan, Z.M., and Zhang, B. (2015). Genetic interaction between NS4A and NS4B for replication of Japanese encephalitis virus. J. Gen. Virol. *96*, 1264–1275.

Liang, Q., Luo, Z., Zeng, J., Chen, W., Foo, S.S., Lee, S.A., Ge, J., Wang, S., Goldman, S.A., Zlokovic, B.V., et al. (2016). Zika Virus NS4A and NS4B Proteins Deregulate Akt-mTOR Signaling in Human Fetal Neural Stem Cells to Inhibit Neurogenesis and Induce Autophagy. Cell Stem Cell *19*, 663–671.

Limpens, R.W., van der Schaar, H.M., Kumar, D., Koster, A.J., Snijder, E.J., van Kuppeveld, F.J., and Bárcena, M. (2011). The transformation of enterovirus replication structures: a three-dimensional study of single- and double-membrane compartments. MBio *2*, e00166–11.

Lindenbach, B.D., and Rice, C.M. (1999). Genetic interaction of flavivirus nonstructural proteins NS1 and NS4A as a determinant of replicase function. J. Virol. *73*, 4611–4621.

Liu, W.J., Wang, X.J., Mokhonov, V.V., Shi, P.-Y., Randall, R., and Khromykh, A.A. (2005). Inhibition of interferon signaling by the New York 99 strain and Kunjin subtype of West Nile virus involves blockage of STAT1 and STAT2 activation by nonstructural proteins. J. Virol. *79*, 1934–1942.

Mackenzie, J.M., Jones, M.K., and Young, P.R. (1996). Immunolocalization of the dengue virus nonstructural glycoprotein NS1 suggests a role in viral RNA replication. Virology *220*, 232–240.

Mackenzie, J.M., Khromykh, A.A., Jones, M.K., and Westaway, E.G. (1998a). Subcellular localization and some biochemical properties of the flavivirus Kunjin nonstructural proteins NS2A and NS4A. Virology *245*, 203–215.

Mackenzie, J.S., Broom, A.K., Hall, R.A., Johansen, C.A., Lindsay, M.D., Phillips, D.A., Ritchie, S.A., Russell, R.C., and Smith, D.W. (1998b). Arboviruses in the Australian region, 1990 to 1998. Commun. Dis. Intell. *22*, 93–100.

Mackenzie, J.M., Jones, M.K., and Westaway, E.G. (1999). Markers for trans-Golgi membranes and the intermediate compartment localize to induced

membranes with distinct replication functions in flavivirus-infected cells. J. Virol. *73*, 9555–9567.

McLean, J.E., Wudzinska, A., Datan, E., Quaglino, D., and Zakeri, Z. (2011). Flavivirus NS4A-induced autophagy protects cells against death and enhances virus replication. J. Biol. Chem. *286*, 22147–22159.

Miller, S., Kastner, S., Krijnse-Locker, J., Bühler, S., and Bartenschlager, R. (2007). The non-structural protein 4A of dengue virus is an integral membrane protein inducing membrane alterations in a 2K-regulated manner. J. Biol. Chem. *282*, 8873–8882.

Miorin, L., Romero-Brey, I., Maiuri, P., Hoppe, S., Krijnse-Locker, J., Bartenschlager, R., and Marcello, A. (2013). Three-dimensional architecture of tick-borne encephalitis virus replication sites and trafficking of the replicated RNA. J. Virol. *87*, 6469–6481.

Moreira, E.F., Jaworski, C.J., and Rodriguez, I.R. (1999). Cloning of a novel member of the reticulon gene family (RTN3): gene structure and chromosomal localization to 11q13. Genomics *58*, 73–81.

Muñoz-Jordan, J.L., Sánchez-Burgos, G.G., Laurent-Rolle, M., and García-Sastre, A. (2003). Inhibition of interferon signaling by dengue virus. Proc. Natl. Acad. Sci. USA *100*, 14333–14338.

Oertle, T., and Schwab, M.E. (2003). Nogo and its paRTNers. Trends Cell Biol. *13*, 187–194.

Oertle, T., Klinger, M., Stuermer, C.A., and Schwab, M.E. (2003). A reticular rhapsody: phylogenic evolution and nomenclature of the RTN/Nogo gene family. FASEB J. *17*, 1238–1247.

Overby, A.K., Popov, V.L., Niedrig, M., and Weber, F. (2010). Tick-borne encephalitis virus delays interferon induction and hides its double-stranded RNA in intracellular membrane vesicles. J. Virol. *84*, 8470–8483.

Patterson, G.H., Piston, D.W., and Barisas, B.G. (2000). Förster distances between green fluorescent protein pairs. Anal. Biochem. *284*, 438–440.

Pautasso, C., Bringhen, S., Cerrato, C., Magarotto, V., and Palumbo, A. (2013). The mechanism of action, pharmacokinetics, and clinical efficacy of carfilzomib for the treatment of multiple myeloma. Expert Opin. Drug Metab. Toxicol. *9*, 1371–1379.

Romero-Brey, I., and Bartenschlager, R. (2016). Endoplasmic Reticulum: The Favorite Intracellular Niche for Viral Replication and Assembly. Viruses *8*, E160.

Roosendaal, J., Westaway, E.G., Khromykh, A., and Mackenzie, J.M. (2006). Regulated cleavages at the West Nile virus NS4A-2K-NS4B junctions play a major role in rearranging cytoplasmic membranes and Golgi trafficking of the NS4A protein. J. Virol. *80*, 4623–4632.

Schlegel, A., Giddings, T.H., Jr., Ladinsky, M.S., and Kirkegaard, K. (1996). Cellular origin and ultrastructure of membranes induced during poliovirus infection. J. Virol. *70*, 6576–6588.

Schwartz, M., Chen, J., Janda, M., Sullivan, M., den Boon, J., and Ahlquist, P. (2002). A positive-strand RNA virus replication complex parallels form and function of retrovirus capsids. Mol. Cell *9*, 505–514.

Stern, O., Hung, Y.-F., Valdau, O., Yaffe, Y., Harris, E., Hoffmann, S., Willbold, D., and Sklan, E.H. (2013). An N-terminal amphipathic helix in dengue virus nonstructural protein 4A mediates oligomerization and is essential for replication. J. Virol. *87*, 4080–4085.

Tanaka, K. (2009). The proteasome: overview of structure and functions. Proc. Jpn. Acad. Ser. B Phys. Biol. Sci. *85*, 12–36.

Tang, W.-F., Yang, S.-Y., Wu, B.-W., Jheng, J.-R., Chen, Y.-L., Shih, C.-H., Lin, K.-H., Lai, H.-C., Tang, P., and Horng, J.-T. (2007). Reticulon 3 binds the 2C protein of enterovirus 71 and is required for viral replication. J. Biol. Chem. *282*, 5888–5898.

Teo, C.S.H., and Chu, J.J.H. (2014). Cellular vimentin regulates construction of dengue virus replication complexes through interaction with NS4A protein. J. Virol. *88*, 1897–1913.

Tolley, N., Sparkes, I., Craddock, C.P., Eastmond, P.J., Runions, J., Hawes, C., and Frigerio, L. (2010). Transmembrane domain length is responsible for the ability of a plant reticulon to shape endoplasmic reticulum tubules in vivo. Plant J. *64*, 411–418.

Voeltz, G.K., Prinz, W.A., Shibata, Y., Rist, J.M., and Rapoport, T.A. (2006). A class of membrane proteins shaping the tubular endoplasmic reticulum. Cell *124*, 573–586.

Wang, R.Y., and Li, K. (2012). Host factors in the replication of positive-strand RNA viruses. Chang Gung Med. J. *35*, 111–124.

Wang, Z., Yang, J., Kirk, C., Fang, Y., Alsina, M., Badros, A., Papadopoulos, K., Wong, A., Woo, T., Bomba, D., et al. (2013). Clinical pharmacokinetics, metabolism, and drug-drug interaction of carfilzomib. Drug Metab. Dispos. *41*, 230–237.

Welsch, S., Miller, S., Romero-Brey, I., Merz, A., Bleck, C.K.E., Walther, P., Fuller, S.D., Antony, C., Krijnse-Locker, J., and Bartenschlager, R. (2009). Composition and Three-Dimensional Architecture of the Dengue Virus Replication and Assembly Sites. Cell Host Microbe *5*, 365–375.

Westaway, E.G., Mackenzie, J.M., Kenney, M.T., Jones, M.K., and Khromykh, A.A. (1997). Ultrastructure of Kunjin virus-infected cells: colocalization of NS1 and NS3 with double-stranded RNA, and of NS2B with NS3, in virus-induced membrane structures. J. Virol. *71*, 6650–6661.

Westaway, E.G., Khromykh, A.A., and Mackenzie, J.M. (1999). Nascent flavivirus RNA colocalized in situ with double-stranded RNA in stable replication complexes. Virology *258*, 108–117.

Westrate, L.M., Lee, J.E., Prinz, W.A., and Voeltz, G.K. (2015). Form follows function: the importance of endoplasmic reticulum shape. Annu. Rev. Biochem. *84*, 791–811.

Wu, M.J., Ke, P.Y., Hsu, J.T.A., Yeh, C.T., and Horng, J.T. (2014). Reticulon 3 interacts with NS4B of the hepatitis C virus and negatively regulates viral replication by disrupting NS4B self-interaction. Cell. Microbiol. *16*, 1603–1618.

Yang, Y.S., and Strittmatter, S.M. (2007). The reticulons: a family of proteins with diverse functions. Genome Biol. *8*, 234.

Zou, J., Xie, X., Wang, Q.Y., Dong, H., Lee, M.Y., Kang, C., Yuan, Z., and Shi, P.Y. (2015). Characterization of dengue virus NS4A and NS4B protein interaction. J. Virol. *89*, 3455–3470.

Zurek, N., Sparks, L., and Voeltz, G. (2011). Reticulon short hairpin transmembrane domains are used to shape ER tubules. Traffic *12*, 28–41.